Springer

Journal of
Mechanical
Science and
Technology

Journal of Mechanical Science and Technology 22 (2008) 157~165

www.springerlink.com/content/1738-494x

Thermally-driven nanoscale pump by molecular dynamics simulation

Minsub Han*

Department of Mechanical Engineering University of Incheon 177 Dohwa-dong, Nam-gu, Incheon, Korea

(Manuscript Received March 2, 2007; Revised July 19, 2007; Accepted July 24, 2007)

Abstract

The feasibility of a device is studied that drives a fluid in nanoscale channel using a phenomenon called thermal transpiration, where the fluid is set in motion by a temperature gradient in the fluid-solid interface. Four different types of systems are considered using the Molecular Dynamics Simulation. They differ mainly in channel configuration and the way the gradient is applied. The simulation results show that the design of the device has major technical obstacles. One is a difficulty in imposing a sufficiently-large temperature gradient in the small scale. In this case, the feature like thermal-contact-resistance at the interface needs to be included in design considerations. The second is a limited flow-development under an increased viscous drag in the narrow channel. One of the considered systems proves to be effective in a pumping operation. The system is based on a unit that repeats itself periodically in the system. The unit is composed of two regions: one that drives a fluid by thermophoretic force and the other that guides the fluid smoothly with little thermophoretic force. The latter region is made of a thermally-insulating, weakly-interacting solid.

Keywords: Thermal transpiration; Thermophoresis; Molecular simulation

1. Introduction

One of the essential components in a typical fluid system is a device to drive fluids with respect to a given purpose. The examples are heart in the circulatory system of mammals, rotary pumps in turbo machinery and piston in an engine. They all provide the given system with a driving means that are necessary to control and manipulate the fluid for various purposes. Recently, enormous attentions are paid to the fluid systems of small scales. The so-called microfluidics, or even nanofluidics, has implications in a wide range of applications in fields of bio-, nano- and environmental technologies [1]. Many factors determining the physics of fluid motion in the small scale are normally not dominant and, in some cases, negligible in a macroscopic scale. Therefore, each component in a fluid system of the small scale would be quite distinctive in its operation, which needs to be closely accounted for in its design. This is also true of a pumping device of the small scale that needs to drive the fluid with control and efficiency.

As the scale becomes smaller, the surface forces like surface tension and viscous force are far more dominant than inertia and body forces. A typical pump design based on the latters may not be the effective way to drive fluid. For example, two of the most popular methods to produce a flow in micro-devices are based on either electro-osmosis or dieletrophoresis. Both methods use the surface force appearing in the electrical double-layer. As practical micro/nano-fluid-systems tend to be fraught with various components performing complicated functions, alternative methods are still needed to complement and improve the aforementioned methods. One of the candidates that deserve more attention is the method based on thermophoretic force. Thermophoretic force occurs when a fluid bounded by a solid is under a temperature gradient tangential to the fluid-solid interface. The force can not be neglected if the temperature gradient and the degree of molecular

*Corresponding author. Tel.: +82 32 770 8411, Fax.: +82 32 770 8410
E-mail address: mhan@incheon.ac.kr
DOI 10.1007/s12206-007-1019-4

interaction between the neighboring phases are of a sufficiently large amount. Phenomena related with thermophoretic force can easily be found in thermal systems of small scales. For example, the phenomenon of thermophoresis can be found in the drift of colloids in thermal boundary layer.

Pump designs using thermophoretic force were already suggested for rarefied gas [2-4]. However, the designs relevant for the micro/nano systems of liquids are rarely studied. Author recently suggests that some pumping operation based on thermophoretic force is indeed possible in nanoscale channels [5]. In this study, the designs of a device that can drive a liquid in a nanoscale channel are presented, and the feasibility and characteristics of each design are discussed in more detail.

2. Theory

2.1 Background

When a fluid is bounded by a solid and a temperature gradient is formed tangentially to the fluid-solid interface, a flow appears near the solid. The flow is not developed by inertia or buoyancy forces. When molecules in the fluid interact with the surface of the solid, some unbalanced force, or thermophoretic force, occurs in the event of the temperature gradient and set the molecules in drift motions. Fig. 1 illustrates the basic mechanism that induces the unbalanced force and, therefore, the flow. The solid and dotted lines in Fig. 1(a) show MD results of the tangential pressure distribution, respectively. The temperatures of the two cases are different, but the pressures far from the solid, $z \rightarrow \infty$, are of the same amount. If we place the two states side by side, we would have no pressure gradient developed in the bulk even in the presence of temperature gradient. However, this situation can not be sustained close to the solid surface where there always exists a pressure difference, shown as the dashed line in Fig. 1a, due to the presence of solid. The pressure difference collectively results in an unbalanced force occurring only in the interfacial region [Fig. 1(b)]. Many phenomena are based on this force: thermal creep flow, thermal edge flow, thermal transpiration and thermophoresis [6]. The studies on the subject in the literature are largely on the fluid system of rarefied gas. Using the physical argument relevant to ideal gas, Maxwell proposed the following relationship [7].

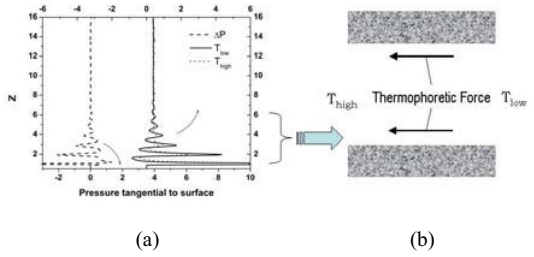

(a) (b)

Fig. 1. Illustration of the origin of thermophoretic force: (a) MD results of the tangential pressures with respect to the distance from the solid surface, (b) the integrated effect of the unbalanced pressure occurring near the surface.

$$V_{th} = a\nabla T \tag{1}$$

For a dilute gas, for example, the proportional factor a depends mainly on the mean-free-path of the gas. However, in the case of liquids, the factor depends more on the characteristics of the dense state like long-range intermolecular forces [8].

Even though it usually has a negligible effect on a macro-scale object in a normal condition, the thermophoretic flow becomes of an amount large enough to drive the entire fluid in some instances. Good examples can be found in rarefied-gas flows and micro/nano-flows. It is so in the latter case because the interfacial force like thermophoretic force becomes a dominant factor owing to the scale of system. When a temperature gradient is applied along the axis of a nanoscale pipe or channel, a significant amount of flow may be induced by thermophoretic force. It may then have a potential to be used for the pumping operation in nanoscale fluid systems.

2.2 System design

To produce a sufficient pumping power, a substantial amount of temperature gradient would be required in the system. However, the gradient cannot be increased indefinitely because a part of the system would eventually be overheated. Also, applying a large gradient requires a good thermal-insulation, which becomes increasingly difficult in the small scales. These difficulties may be overcome by connecting a single pumping unit of a modest gradient with another in sequence. Assembling a large number of the units would provide a necessary pumping power with less limitation.

A system of the units repeating in sequence results

in a periodic temperature distribution, and the sign of the temperature gradient alternates along the flow. In the unit design, the thermophoretic force is maximized in some region of the temperature gradient of certain sign and is suppressed in other region of the opposite sign. This situation is illustrated in Fig. 2. Fig. 2(a) shows the system that consists of the walls interacting with the fluid only strongly. The sign of the temperature gradient alternates periodically in the flow direction and so does the sign of the thermophoretic force. Therefore, the net flow developed by the forces would be largely cancelled out. The situation is similar in Fig. 2(b) where the signs of the temperature gradient and the thermophoretic force also alternate periodically. However, we may reduce a significant amount of thermophoretic force using a weakly-interacting wall or fluid in the region of temperature gradient of a certain sign, for example, minus in this case. Then, a larger amount of flow is developed by the forces in the region of temperature gradient of the opposite sign, plus in this case, and the net flow would be of a significant amount.

Four types of models are considered in which these ideas are implemented. The first two models are based on similar ideas found in the literature [2, 3]. In the first system, Model I, the fins of high and low temperatures are distributed in such a way that the thermal-edge flow is induced [Fig. 3(a)]. In the next, Model II, the channels of two different temperatures are located side by side and the two channels are bounded by the bulk liquid [Fig. 3(b)]. In the third and fourth systems, Model III and IV, a non-conducting slipping wall is chosen in the region of one gradient and the normal wall is used in the region of the opposite gradient [Fig. 3(c) and 3(d)]. In Model III, the temperature gradient is imposed by heat source and sink. In Model IV, it is imposed by walls controlled to given temperatures.

Some comments may be made on a possibility of dielectric effect in the last model. One of the common ways of controlling the temperature of a small-scale device is to control the heating by electric current. If we use the electrically-conducting material like Pt as, for example, a channel wall and apply an electric field there, the fluid as well as the channel wall can easily be heated. It is then possible that some of the applied electric-field is also effective in the fluid region. If the fluid is not neutral, for example, a solvent containing ions, this may induce some electro-osmotic flow. Even when the fluid is completely neutral, a non-uniform electric field may induce some flow of a dielectrophoretic origin. These flows may complicate the operation of the pump based on thermophoretic forces. However, they may be lessened significantly,

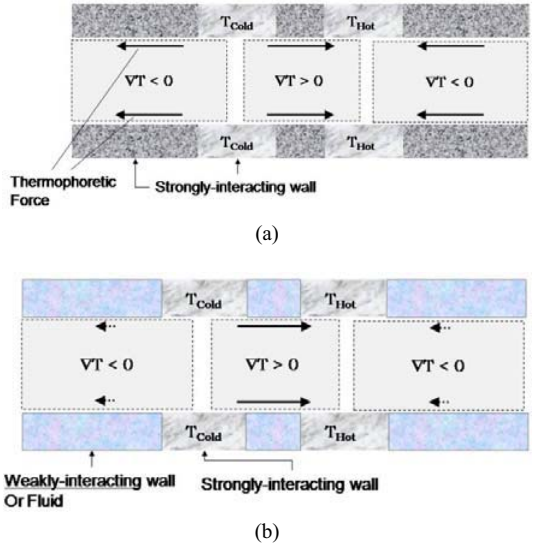

Fig. 2. Schematic of two different periodic fluid-systems: (a) the system of strongly-interacting walls only, (b) the system of walls composed of weakly-interacting walls as well as strongly-interacting walls.

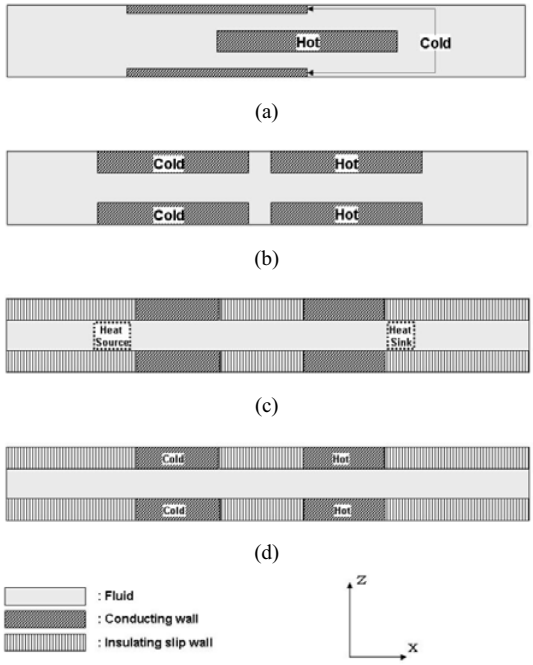

Fig. 3. Schematic of four different fluid systems: (a) Model I, (b) Model II, (c) Model III and (d) Model IV.

if not removed completely, in a relatively simple manner. The intended temperature distribution is required only in the liquid region very close to the solid, the liquid-solid interfacial region. Therefore, the electric field can be applied to a solid region sufficiently far from the liquid using the solid of a high thermal conductivity, such as Pt, and the effect of the field could be made sufficiently weak on the liquid.

3. Method

The non-equilibrium molecular dynamics simulation (NEMD) is performed in this study. The major part of the simulation system consists of liquid argon and platinum wall. The argon atoms interact with each other through the pairwise intermolecular potential of a truncated and shifted Lennard-Jones (LJ) 6-12 potential.

$$U = \begin{cases} U_{LJ}(r) - U_{LJ}(r_c) & \text{if } r < r_c, \\ 0 & \text{otherwise,} \end{cases} \quad (2)$$

where

$$U_{LJ}(r) = 4\varepsilon\left[\left(\frac{r}{\sigma}\right)^{12} - \left(\frac{r}{\sigma}\right)^{6}\right] \quad (3)$$

and $r_c = 3\sigma_{Ar}$. The properties of argon are given in the footnote of Table 1. The atoms of argon and platinum also interact with the pairwise potential U_{LJ} with $\sigma_{Ar-Pt} = 1.1935\sigma_{Ar}$ and $\varepsilon_{Ar-Pt} = 0.4211\varepsilon_{Ar}$, which values are obtained by fitting the angular and velocity distribution of an argon atom scattered from a platinum surface [9]. More accurate representations of the interaction exist in the literature, and they are more time-consuming [10, 11]. A harmonic potential is used for the atom-atom interactions in the Pt lattice.
Table 1.

$$U_{harmonic}(r) = \frac{1}{2}k\left(r - r_o\right)^2 \quad (4)$$

where $r_o (= 0.8248\sigma_{Ar})$ is the distance between nearest two atoms in FCC lattice (111) of Pt. The spring constant is given as $k = 3239.569\varepsilon_{Ar}/\left(\sigma_{Ar}\right)^2$, which, in combination with the ghost particle scheme for temperature control explained below, represents the bulk phonon-spectra quite well [9, 10, 12]. Also, the thermally-insulating slip wall is introduced, and their atoms are fixed in space in the same FCC lattice and interact with fluid atoms through only the repulsive potential, for which $r_c = 2^{1/6}\sigma_{Ar-Pt}$. The periodic boundary condition is applied in all directions.

Table 1. The reduced properties for Lennard-Jones system†

Reduced property	Dimensional representation
Density(ρ^*)	$\rho\sigma_{Ar}^{\ 3}$
Energy(ϕ^*)	ϕ/ε_{Ar}
Flux(F^*)	$F/(\varepsilon_{Ar}^{\ 1/2}\sigma_{Ar}^{\ -3})$
Length(r^*)	r/σ_{Ar}
Temperature(T^*)	$k_B T/\varepsilon_{Ar}$
Time(t^*)	$t\varepsilon_{Ar}^{\ 1/2}/\sigma_{Ar}$

†k_B: Boltzman Constant, σ_{Ar} = 3.4 Å, ε_{Ar}/k_B = 120 K.

The equations of motions are integrated using the velocity Verlet algorithm [13] and the time step of $\Delta t = 0.001\sigma_{Ar}\varepsilon_{Ar}^{\ -1/2}$ is used. When the temperature of the Pt walls needs to be controlled, as in the cases of Model IV, the scheme based on the so-called ghost particle is used that lets the energy in and out to maintain a constant temperature [14]. The ghost particles are located in boundaries of the simulation system and play the role of a thermal reservoir, or a semi-infinite solid phase of a given temperature. A more details on implementation can be found in the literature [13, 15]. The heat source and sink in the system are simulated by scaling the velocities of atoms. At each 60th step, the same amount of kinetic energies are added in the heat-source region and subtracted in the heat sink. Only the velocity components in y and z directions, which are normal to the flow, are involved in the scaling to minimize the influence on particle drift.

The initial positions of solid atoms are those of zero degree Kelvin. The initial positions of fluid atoms are chosen randomly on condition that the distance from the nearest atom is larger than $0.5\sigma_{Ar}$. The initial velocities are chosen randomly from the Gaussian distribution. The initial system is equilibrated during 2×10^5 steps. The data are collected at every 50th step, and the collected data are averaged at every 1×10^4 th step. The numbers of bins for data collection and average are 210 and 70 in x and z directions, respectively.

4. Result and discussion

The dimensional units of the results presented in

this section are all reduced with respect to properties of argon (See Table 1.) if not indicated otherwise. The first two systems in consideration are illustrated in Figs. 4(a) and 4(b). A typical geometry of the simulations for Model I is shown in Fig. 4(a). The walls in the same horizontal position are controlled to the same temperature in this periodic system. The wall located in the middle of the z direction is controlled to a temperature higher than those of other two walls. Such parameters as the gap between the walls, pitch, wall-length and temperature-difference between the walls are varied to some degree to test the feasibility of the design. However, any of the simulated cases do not develop a significant amount of flow. Fig. 5 shows a typical result in the simulation for Model I. The length of the wall is about 41.47 and the pitch between the "hot" and "cold" walls is about 21.33. The temperatures of the walls are 1.4 and 1.0, respectively. In Fig. 5(a), the density distribution shows that the fluid near the solid surfaces develops some layered structure. This is notable especially in the region between the solid surfaces. The temperature gradient is formed between the walls. However, the gradient is mostly located in a-couple-of-diameter-thick interfacial region and vaguely noticeable in the bulk liquid. This is due to the so-called thermal contact resistance in the interface. The difference in the molecular structure between the phases tends to hinder the transport of energy carried by phonon in their interface and results in a lower thermal conductance. The temperature gradient in the liquid region between the solid surfaces does not measure up to a significant amount. It is mainly because the gradient is developed only in local regions near the edges. Also, the temperature gradient developed is tilted about 45 degrees to the intended direction, x, of the flow. In all, no significant amount of flow appears that has globally consistent direction [Fig. 5(c)].

In the second design of Model II [Fig. 4(b)], the hot and cold walls are placed side by side to form a continuing channel. The two pairs of the walls, an upper pair and a lower, are not in complete contact and there exist a couple of fluid layers. This layer enables a large gradient in a close distance taking advantage of the thermal contact resistance. Compared to Model I, the thermal gradient in Model II is formed in a relatively large area and in the same direction as that of the intended flow. In simulation, various sets of parameters are also varied such as temperatures of walls, gap between the walls and width of the channel. Fig.

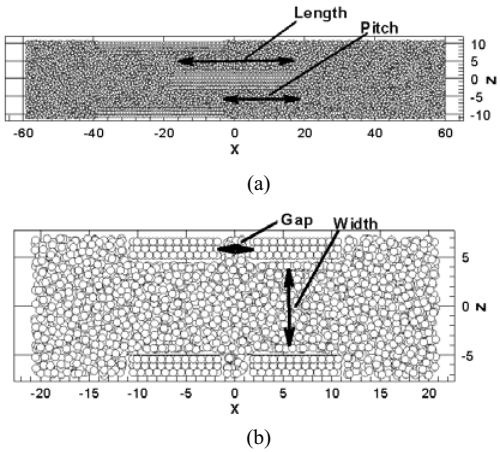

Fig. 4. Snapshots of (a) Model I and (b) Model II systems.

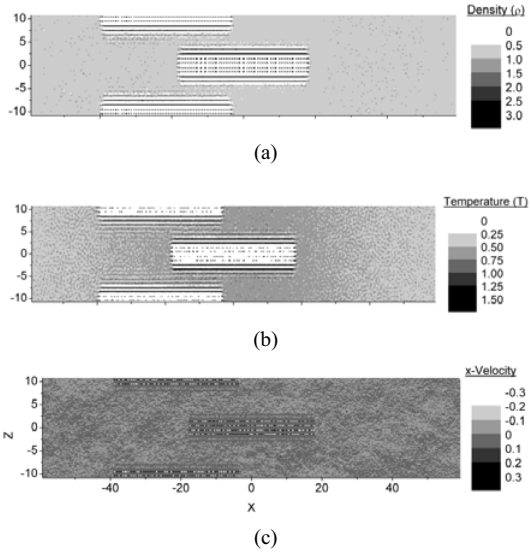

Fig. 5. Simulation results of Model I.

6 shows the results of a simulation case in which the initial fluid density is 0.86, temperature 0.9 and 0.8, gap width 4 and channel width 6. The velocity distri bution shows that there is no systematic development of flow, either. If some flows may occur locally in the channel, they are not clearly seen in the bulk liquid. Some bubble also occurs occasionally in the bulk and blocks the flow depending on the temperature condition.

Major improvement is made in next two designs where the thermally-insulating slip, or TIS, wall is introduced. First, the "thermally-insulating" wall simulates a material that does not transport energy by phonon, and is modeled as a lattice whose particles

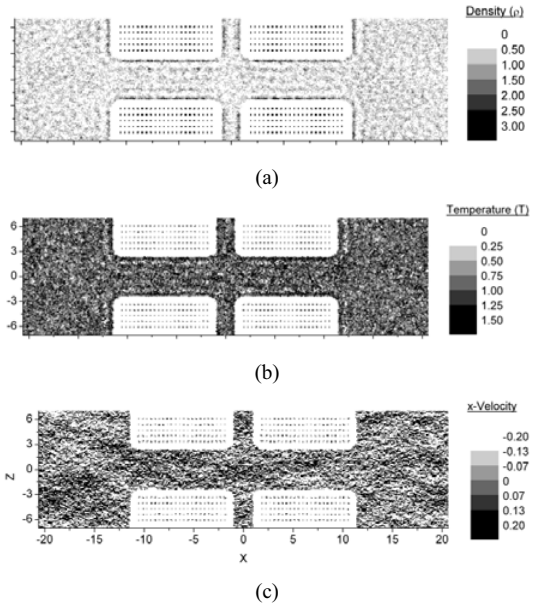

Fig. 6. Simulation results of Model II.

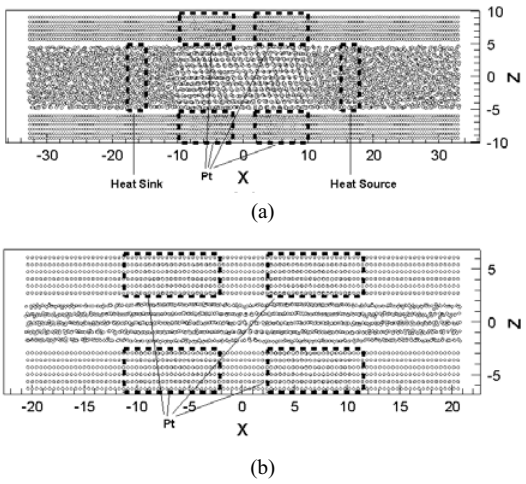

Fig. 7. Snapshot of the simulation systems of (a) Model III and (b) Model IV.

Table 2. Simulation cases for Model III.

Case	Energy In/Out Rate ($\varepsilon^{3/2}\sigma$)	Channel width (σ)	Initial fluid Density ($1/\sigma^3$)	No. flowrate $\times 10^4(\varepsilon^{1/2}\,\sigma^{-1})$	No. flux $\times 10^6(\varepsilon^{1/2}\,\sigma^{-3})$
1	138.83	4	0.8	1.90	6.65
2	138.83	4	0.9	-3.07	-10.74
3	277.83	5	0.9	1.97	5.52
4	138.83	5	0.9	2.28	2.28
5	138.83	6	0.9	4.12	5.31
6	138.83	7	0.9	0.925	1.85
7	138.83	9	0.9	7.7	11.98
8	138.83	11	0.9	-6.25	-7.95
9	138.83	7	0.8	5.1	10.20
10	138.83	9	0.8	11.675	18.16
11	138.83	11	0.8	15.1	19.22

are fixed in space. More importantly, the "slip" wall implies a solid whose molecular potential attracts fluid atoms weakly, and it is modeled with a repulsive potential in simulation. The TIS wall has some characteristics that are beneficial in design. First, since the wall interacts with fluids weakly, thermophoretic force thus induced is of a small amount. It does not conduct heat and, therefore, does not disrupt a given temperature distribution largely set up by other part of the system. In all, while it has a minimal effect on the fluid, TIS wall can smoothly guide the fluid flow developed elsewhere. In Figs. 7(c) and 7(d), the walls are composed of the TIS walls if they are not indicated as a platinum wall, and the walls are located in such a way to use the above features. That is, the TIS walls are located in the region where the sign of temperature gradient is opposite to that in the region of Pt walls. The interactions in the region of Pt walls are the direct source of the fluid motion while the fluid is just guided smoothly with minimal interaction in the region of TIS walls. Also, the TIS walls sandwiched between the Pt walls enable a large temperature gradient in a short distance.

In the Model III of Fig. 3(c), the heat source and sink are used to impose the temperature gradient. They are physically analogous to the exothermic and endothermic reaction processes respectively. From the simulation point of view, the heat source and sink are one of robust means to impose and control the temperature gradient in the system. The typical simulation system is shown in Fig. 7(a) where a snapshot of the simulation for Case 11 in Table 2 is presented. The diameter of atoms is shrunk from the real size intentionally to underscore the structure of phase states, and the locations of the heat source and sink are indicated with dashed lines. The locations of the platinum walls are also indicated, and the rest of the walls are TIS walls. It is clearly noticeable that the liquid between Pt walls are highly structured, which would enhance the energy transfer. Typical properties of the model are shown in Fig. 8. At the heat source

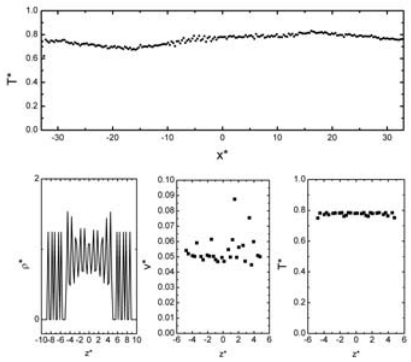

Fig. 8. Simulation results for Model III: Case 11 in Table 2.

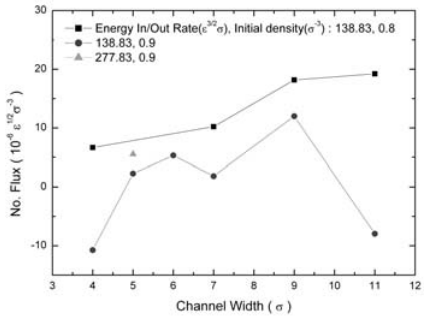

Fig. 9. The number flux results for various cases of Model III.

and sink regions, the energy input and output are of a constant rate and a same amount and, therefore, there is no net energy flux into the simulation system. The uppermost Fig. is obtained by averaging the temperature over the fluid atoms in the same x positions. Similarly, the rest of Figs are obtained by averaging over the atoms in the same z positions. More information on the conditions applied in the cases is provided in Table 2. A positive temperature gradient in the x direction is developed in the region of Pt walls. The negative temperature gradient is located in the regions elsewhere in which only TIS walls exist. The particle flux is developed in the x direction. The velocity profile is close to that of the plug flow, which typically occurs in phoretic flows. That is, the velocity profile is more or less flat in most of the inner region and a simple shear flow occurs only in the fluid-solid interfacial region. It is because, as in any other phoretic flows, the source of fluid motion is located in the interfacial region. The fluid is highly structured owing to the proximity to the solid walls. The values like energy input/output, channel width and fluid density are varied in the simulation, and the number flux results are compared in Fig. 9. In the simulated cases,

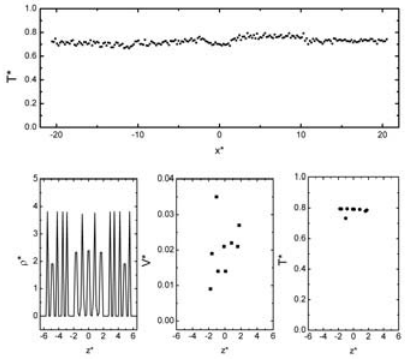

Fig. 10. Simulation results for Model IV.

Table 3. Simulation cases for Model IV.

Case; time steps(10^2)	Heating Values	Channel width (σ)	Density ($1/\sigma^3$)	No. flowrate× $10^4(\varepsilon^{1/2}\,\sigma^{-1})$	No. flowrate× $10^6(\varepsilon^{1/2}\,\sigma^{-3})$
1i; 0~2	T^*_{hot}=1.1, T^*_{cold}=0.8	5	0.8	0.15	0.41
1ii; 2~4	〃	5	0.8	0.25	0.70
1iii; 4~6	〃	5	0.8	-0.525	-1.47
1iv; 6~8	〃	5	0.8	-0.35	-0.98
2i; 0~2	〃	4	0.9	0.16	0.56
2ii; 2~4	〃	4	0.9	0.68	2.38
2iii; 4~6	〃	4	0.9	1.63	5.70
2iv; 6~8	〃	4	0.9	1.65	5.77
3i; 0~2	〃	5	0.9	-1.27	-3.56
3ii; 2~4	〃	5	0.9	-1.58	-4.42
3iii; 4~6	〃	5	0.9	0.13	0.36
3iv; 6~8	〃	5	0.9	0.625	1.75

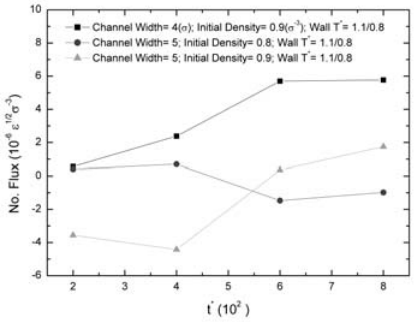

Fig. 11. The number flux results for various cases of Model IV.

flows are consistently developed, mostly in the x direction. The number flux is of about the order of 10^5 and tends to increase with a larger value of heat

source and sink. The flows in the opposite direction are also observed. The flow direction in x-direction is expected in the theory of thermal transpiration for the given temperature distribution. The cases of the flow of a negative x-direction belong to the high density cases, 0.9, and may be related with the solid-like structure developed in the interfacial region. The cases of a lower density, 0.8, do not show this feature. The trends are also shown that a higher flux is produced when the fluid is of a relatively lower density and the channel is of a larger width. This may indicate that even though the case of a high fluid density and smaller channel width induce a higher thermophoretic forces in a given condition, a high viscous force also arises and impedes the fluid motion.

Finally, in the Model IV of Fig. 3d, the temperature gradient is imposed by the walls of different temperatures respectively. Controlling wall temperature may be less effective method to impose the gradient than using the heat sources because of thermal contact resistance. On the other hand, it may be more practical method to design a device. The results are shown in Fig. 10 for the case 2ii in Table 3. The data are again averaged as the way Fig. 8 is produced. The temperature gradient developed here is smaller than the case using heat sources and so is the amount of flow developed. The density and velocity profiles show similar characteristics as before. The fluid density is structured, and it is more so because the channel is narrower. The velocity profile also follows that of the plug flow. The simulated cases indicate that the present design is slower and less robust in development of the flow. Fig. 11 shows that it requires as much as an order more time to stabilize the flow and the flow direction is sensitive to the channel width and the fluid density.

5. Conclusions

The design of a device that can drive the liquid in a nanoscale channel is studied using Molecular Dynamics Simulation. The device utilizes the thermophoretic force that occurs in fluid-solid interfacial region in the presence of a temperature gradient applied tangentially to the interface. Four different types of systems are considered. The systems are based on a periodically-repeating unit. In the unit, various channel arrangements and methods of applying the gradient are considered to maximize the pumping effect.

The design of a pumping system in nanoscale channel using thermophoretic force needs to overcome a number of obstacles. First, it is difficult to impose a large amount of temperature gradient not only because of the small scale but because controlling the temperature by wall-heating becomes less effective owing to thermal contact resistance. Also, since the interfacial region occupies significant portion of the channel, the viscous drag tends to increase at the same time the thermophoretic force increases. Finally, the system based on a periodically-repeating unit must have regions of both a positive temperature gradient and a negative. The thermophoretic force in either one of the regions must be weakened, if not removed.

One of the systems in consideration turns out to show a significant pumping effect. It has an element that may relieve some of the aforementioned difficulties: the thermally-insulating slip (TIS) wall. The TIS wall is an idealized model of a solid material that conducts little heat and interacts weakly with fluid molecules. It can help setting up a large temperature gradient with minimal disturbance, and also can guide the developed flow more seamlessly.

Finally, some of the characteristics of flow development in the channel are discussed. The heating method, channel width and density of fluid are varied in the simulated cases. The results indicate that as the size of system comes close to that of interfacial region, various characteristics of interface start to show up in the flow development process and needs to be taken into account in the design. They include structuring of fluid, higher viscosity and thermal contact resistance.

Acknowledgement

This work was supported by the University of Incheon Reserch Grant in 2006.

Nomenclature

T : Temperature
U : Intermolecular potential
V_{th} : Thermophoretic velocity of particle
a : Proportional factor
k : Spring constant
r : Distance between two atoms
t : Time

Greek symbols

σ : Molecular diameter

ε : Molecular interaction energy

Subscripts

th : Thermophoretic
LJ : Lennard-Jones
o : Initial particle position
c : Cut-off
Ar : Argon
Ar-Pt : Between argon and platinum
harmonic : Harmonic potential

Superscripts

* : Reduced with respect to argon properties

References

[1] H. A. Stone, A. D. Stroock and A. Ajdari, Engineering Flows in Small Devices: Microfluidics Toward a Lab-on-a-Chip *Ann. Rev. Fluid Mech.* 36 (2004) 381.

[2] H. Sugimoto and Y. Sone, Vacuum pump without a moving part driven by thermal edge flow *Rarefied Gas Dynamics*, eds. M. Capitelli, American Institute Of Aeronautics (2003) 168.

[3] Y. Sone, Y. Waniguchi and K. Aoki, One-way flow of a rarefied gas induced in a channel with a periodic temperature distribution *Phys. Fluids*, 8 (1997) 2227.

[4] Y. Sone and H. Sugimoto, Vacuum pump without a moving part and its performance *Rarefied Gas Dynamics* eds. A.D. Ketsdever and E.P. Muntz , American Institute Of Aeronautics (2003) 1041

[5] M. Han, Molecular Dynamics Simulation of Nanoscale Liquid Pump Driven by Temperature Gradient, Proceedings of Asia Pacific Conference on Optics Manufacture, Hong Kong, (2007) 183.

[6] Y. Sone, Flows Induced by Temperature Fields in a Rarefied Gas and their Ghost Effect on the Behavior of a Gas in the Continuum Limit *Ann. Rev. Fluid Mech.* 32 (2000) 779.

[7] J. C. Maxwell and J. C., On the stress in rarefied gases arising from inequalities of temperature *Phil. Trans. Roy. Soc. London* 170 (1879) 231.

[8] M. Han, Thermophoresis in liquids: a molecular dynamics simulation study *J. Colloid Inter. Sci.* 284 (2005) 339.

[9] G. Q. Xu, S. L. Bernasek and J. C. Tully, Stochastic trajectory studies of small argon cluster scattering from Pt(111) *J. Chem. Phys.* 88 (1988) 3376.

[10] M. Head-Gordon, J. C. Tully, C. T. Rettner, C. B. Mullins and D. J. Auerbach, On the nature of trapping and desorption at high surface temperatures. Theory and experiments for the Ar-Pt(111) system *J. Chem. Phys.* 94 (1991) 1516.

[11] C. Ramseyer, P. N. M. Hoang and C. Girardet, Interpretation of high-order commensurate phases for an argon monolayer adsorbed on Pt(111) *Phys. Rev. B*, 49 (4) (1994) 2861-2868.

[12] C. R. Arumainayagam, R. J. Madix, M. C. McMaster, V. M. Suzawa and J. C. Tully, Trapping dynamics of Xenon on Pt(111) *Surf. Sci.*, 226, (1990) 180.

[13] M. P. Allen and D. J. Tildesley, Computer Simulation of Liquids, Oxford University Press, Oxford, (1987)

[14] J. C. Tully, Dynamics of gas-surface interactions: 3D generalized Langevin model applied to fcc and bcc surfaces *J. Chem. Phys.* 73 (1980) 1975-1985.

[15] M. Han, J. S. Lee, S. Park, and Y. K. Choi, Molecular dynamics study of thin film instability and nanostructure formation *Int. J. Heat Mass Transfer* 49 (2006) 879-888.

[16] P. Yi, D. Poulikakos, J. Walther and G. Yadigaroglu Molecular dynamics simulation of vaporization of an ultra-thin liquid argon layer on a surface *Int. J. Heat Mass Transfer* 45 (2002) 2087-2100.